XL CILAMCE
IBERO-LATIN AMERICAN CONGRESS ON COMPUTATIONAL METHODS IN ENGINEERING
NOVEMBER 11-14, 2019
Praiamar Natal Hotel & Convention
Natal, RN-BRAZIL

A 1DBEM/BEM COUPLING FORMULATION APPLIED TO REINFORCED VISCOELASTIC DOMAINS

Antonio Rodrigues Neto[a]
Edson Denner Leonel[a]
antonio.rodrigues.neto@usp.br
edleonel@usp.br
[a] *University of São Paulo, São Carlos School of Engineering, Department of Structural Engineering – Av. Trabalhador São Carlense, 400, 13566-590, São Carlos - SP, Brazil.*

Abstract. This work presents a numerical formulation based on the Boundary Element Method (BEM) for the mechanical analysis of reinforced viscoelastic materials. The reinforced domain is represented by a numerical methods coupling technique, in which the material matrix is modelled by the usual two-dimensional singular BEM formulation and a one-dimensional approach of the BEM, called 1DBEM, is used for the reinforcements. The 1DBEM is based on an axial fundamental solution for elastic 1D domains, easily found in the literature. No relative displacements between matrix and reinforcements are considered to formulate the coupling and the contact force is a one-dimensional load distributed along the reinforcement's line, which define this 1DBEM/BEM coupling as an alternative to the usual FEM/BEM coupling. The viscoelastic response is added to the matrix behavior, using the Kelvin-Voigt rheological model in the two-dimensional BEM formulation. This approach enables introducing the time-dependent material properties without the need for cells within the domain or convolution integrals. A time discretization is needed to solve the resulting time-dependent equation. However, as previously mentioned in the literature, this approach shows a good convergence behavior regarding the time step size. Finally, the proposed formulation is able to represent reinforced domains with a viscoelastic matrix, such as reinforced structures or fiber-reinforced materials. Numerical applications exhibit the convergence of the model and compare the answer obtained with both 1DBEM/BEM coupling and FEM/BEM coupling techniques with reference results, available in the literature. The results obtained are stable and accurate, which demonstrates the robustness of the formulation proposed in this work.

Keywords: Reinforced domains, Viscoelasticity, BEM/BEM, FEM/BEM

1 Introduction

In recent decades, the human being and the society have evolved significantly. Then, advanced manufactures and products are in constant process of evolution, which lead to the development of complex materials compositions and methods for its mechanical analysis. For example, the structural design of mechanical components and structures using reinforced domains and viscoelastic materials, such as composites, polymers and even concrete, has become crucial in several engineering fields. Considering the search for projects and components mechanically efficient, i.e., high strength with low weight, applications like these ones can be seen as a smart solution in different areas, such as civil engineering, automotive, naval and aeronautics, as mentioned by Armentani and Citarella [1] and Citarella [2]. In the context of mechanical analysis of these complex materials and structures, the analytical approaches available are highly restricted and limited, especially concerning geometries and boundary conditions. As a result, the robust mechanical modelling of complex problems requires the application of numerical approaches. Among the numerical methods available for the mechanical analysis, the Boundary Element Method (BEM) is established and widely utilized. Its advantages, as the mesh dimensionality reduction and the accuracy in representing stress concentration, make the BEM recommended for some mechanical applications, as fracture mechanics problem, infinite domains and viscoelasticity (Oliveira and Leonel [3]).

The viscoelastic materials present both elastic and viscous properties, which cause a time dependent mechanical behavior. Chern [4] and Shaw et al. [5] present a good background about classic approaches to represent the viscoelastic behaviour, which are usually based on relaxation functions and incremental schemes. Classical BEM mathematical formulations were also developed to solve viscoelastic problems, with the use of the principle of correspondence and transformations (Rizzo and Shippy [6]; Liu and Antes [7]; Lee and Westmann [8]). This study applies and alternative BEM formulation for viscoelasticity, proposed by Mesquita and Coda [9, 10, 11]. Based on differential constitutive relations of rheological models, such as Kelvin-Voigt, and the weighted residual technique, this formulation provides a representation for viscoelastic domains by integral equations written exclusively with time-differential boundary equations. This aspect of this approach contributes as an advantage for the using of the BEM, maintaining the mesh dimensionality reduction for the viscoelastic problem. The time derivative terms are approximately evaluated by the finite differences technique, which leads to a time marching process. As mentioned in the literature, this approach shows a good convergence behavior regarding the step size of the time discretization.

On the other hand, modelling reinforced materials and structures usually deals with two different structural elements, which can be modelled differently, such as plane stress or plane strain plates, trusses or beams, for instance. Therefore, a numerical model based on the coupling of different numerical methods, such as the BEM and the Finite Element Method (FEM), seems to be an interesting approach for addressing consistently this problem. Thus, each numerical method can be applied in the modelling of the sub-structure in which it presents best performance. The FEM/BEM coupling was proposed initially by Zienkiewicz, Kelly e Bettes [12]. Since then, several authors have developed new researches based on this coupling technique, making it a consolidated approach. A state of art on this subject is presented by Ganguly, Layton and Balakrishna [13] and Elleithy, Tanaka and Guzik [14]. Furthermore, Bia et al. [15] mentions limitations and advantages of such type of coupling. This approach have been also used coupled with the BEM formulation based on viscoelastic rheological models by Mesquita and Coda [16].

In this context, this study presents a numerical formulation for the mechanical modelling of reinforced viscoelastic domains. The coupling technique for matrix/reinforcement representation is based on the established FEM/BEM coupling. However, a one-dimensional BEM approach is utilized into the reinforcements (1DBEM), which characterizes an alternative BEM/BEM coupling technique, called 1DBEM/BEM. The use of this approach can also be found in Buffon [17], for linear-elastic problems. The linear viscoelastic behavior of the matrix is represented in the two-dimensional BEM formulation by imposing properly the constitutive relations of the rheological model of Kelvin-Voigt.

This approach enables introducing the viscoelastic behavior into the material matrix, whereas the reinforcements still have an elastic constitutive relation. Thus, finite differences technique is applied in the time differential equation, which leads to a time marching process that determines the unknown variables at the boundary, at the reinforcements and its variation along time. The entire problem can be described only by boundary elements, without the need for cells or domain mesh, which provides a stable and robust numerical model to represent reinforced viscoelastic materials. The following items describe the formulation of the proposed model. One application is utilized to demonstrate the accuracy and robustness of the proposed formulation.

2 Review of rheological models: Kelvin-Voigt viscoelastic model

Rheological models defined in the uniaxial space is an approach adopted to describe the mechanical behavior of viscoelastic materials. This technique is based on an analogy with electrical circuit's theory, using idealized simple elements (dashpots and springs) to represent specific mechanical characteristics (Tschoegl [18]). The spring element represents the elastic response and the dashpots represent the viscous response. By the convenient composition of these elements, one can represent different viscoelastic behaviors. A parallel association of one dashpot and one spring represents the Kelvin-Voigt model, as illustrated in Fig. 1.

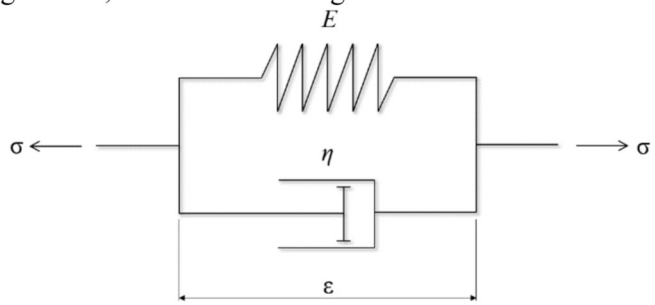

Figure 1: Association schemes of Kevin-Voigt rheological model.

For this model, equilibrium and compatibility equations can be stated as:

$$\begin{aligned} \varepsilon_{ij} &= \varepsilon_{ij}^{(el)} = \varepsilon_{ij}^{(v)} \\ \sigma_{ij} &= \sigma_{ij}^{(el)} + \sigma_{ij}^{(v)} \end{aligned} \quad . \tag{1}$$

In which σ_{ij} and ε_{ij} are the stress and strain tensors. Subscripts '(el)' and '(v)' represent its elastic and viscous parts, respectively.

Elastic and viscous stress can be written in terms of strain components as follows:

$$\begin{aligned} \sigma_{ij}^{(el)} &= C_{ijkl}\varepsilon_{kl} \\ \sigma_{ij}^{(v)} &= \eta_{ijkl}\dot{\varepsilon}_{kl} \end{aligned} \quad . \tag{2}$$

Where the dot symbol represents the temporal derivative, C_{ijkl} and η_{ijkl} are the elastic and viscous constitutive tensors, respectively. Mesquita and Coda [9, 10, 11] presented a proportionality condition between these tensors, given by a single viscoelastic parameter γ and written as follows:

$$\eta_{ijkl} = \gamma C_{ijkl} \quad . \tag{3}$$

Applying Eq. (2) and Eq. (3) into the equilibrium relation given by Eq. (1), one can express the general constitutive relation for Kelvin-Voigt viscoelastic model:

$$\sigma_{ij} = C_{ijkl}\varepsilon_{kl} + \gamma C_{ijkl}\dot{\varepsilon}_{kl} \ . \tag{4}$$

3 BEM integral equations

The integral equation required by the BEM in elastostatics is obtained following the weighting residual technique, as presented in Brebbia, Telles and Wrobel [19]. In this technique, the differential equilibrium equation is weighted by a proper function, assumed to be the fundamental problem solution. So, for 2D elasticity problems, one can write:

$$\int_{\Omega}\left(\sigma_{ij,j} + b_i\right)u_{ki}^{*}d\Omega = 0 \ . \tag{5}$$

Where u_{ki}^{*} is the Kelvin fundamental solution for displacements, which can be found in Brebbia and Dominguez [20], and b_i are the body forces.

Applying the divergence theorem and the elasticity relations of the fundamental problem, Eq. (5) turns into:

$$\int_{\Gamma}u_{ki}^{*}p_i d\Gamma - \int_{\Omega}\varepsilon_{kij}^{*}\sigma_{ij}d\Omega + \int_{\Omega}u_{ki}^{*}b_i d\Omega = 0 \ . \tag{6}$$

In which u_i and p_i are the displacements and tractions at the body's boundary, respectively, and ε_{kij}^{*} is the fundamental solution for strain. Equation (6) is the starting point to obtain the 2D BEM integral representation for viscoelastic analysis, which will be represent in the next item.

To write the 1DBEM integral equation, a one-dimensional homogeneous elastic domain is considered. For this case, one writes the weighting residual expression as follows:

$$\int_{0}^{L}\left(EAu_{,ii} + p\right)u^{*}dx = 0 \ . \tag{7}$$

Where E is the Young modulus, A is the cross-sectional area, p is the distributed load applied along the axial direction and i indicates the axial direction.

Equation (7) exhibits the equilibrium equation weighted by the fundamental problem solution for displacements u^{*}. One must consider a Dirac function applied at a source point (s) as the applied force p in a one-dimensional domain to obtain the fundamental problem of this case. Thus, the fundamental solutions for axial displacement u^{*} and internal force N^{*} at a given field point (f) can be written as follows:

$$\begin{aligned} u_{sf}^{*} &= \frac{|x_f - x_s|}{2EA} \\ N_{sf}^{*} &= -\frac{sign(x_f - x_s)}{2} \end{aligned} \ . \tag{8}$$

In which x_f and x_s are the axial coordinates of the field point and source point, respectively, and $sign(\ )$ is the sign function, i.e., equal to –1 if the argument is negative or 1 otherwise.

Therefore, applying twice the divergence theorem and the equilibrium equation of the fundamental problem in Eq. (7), one writes:

$$u_i - N_{i1}^{*}u_1 + N_{iL}^{*}u_L = u_{i1}^{*}N_1 + u_{iL}^{*}N_L + \int_{0}^{L}\phi_k u_{ik}^{*}p_k dx \ . \tag{9}$$

In which subscripts 1 and L represent the element endpoints and i indicates a given point positioned into the domain. The domain integration represent the distributed load p through the multiplication of its nodal values p_k by the shape functions ϕ_k of one-dimensional elements (similar as

in FEM techniques).

In fact, the boundary is composed of only the endpoints i=1 and i=L in Eq. (9). Any other value for i leads to the internal point equation. However, internal points are considered in the system in order to improve the distributed load (p) representation. Therefore, high-order one-dimensional BEM elements are available in this formulation.

Equation (9) can be generically written in its algebraic form as follows:

$$\mathbf{H_E u_E} = \mathbf{G_E n_E} + \bar{\mathbf{G}}_\mathbf{E} \mathbf{f_E} \ . \tag{10}$$

Where the vectors $\mathbf{u_E}$, $\mathbf{n_E}$ and $\mathbf{f_E}$ contain, respectively, the nodal displacements, concentrated applied forces and distributed axial load nodal values. The matrixes $\mathbf{H_E}$, $\mathbf{G_E}$ and $\bar{\mathbf{G}}_\mathbf{E}$ represent, respectively, the integral results of the fundamental solutions N*, u* and the integral of the fundamental solution u^* multiplied by the shape functions.

Multiplying Eq. (10) by the inverse of $\mathbf{G_E}$ and considering null concentrated applied forces, one can writes the final algebraic form of the 1DBEM, which will be utilized by the coupling formulation, as follows:

$$\left(\mathbf{G_E}\right)^{-1} \mathbf{H_E u_E} = \left(\mathbf{G_E}\right)^{-1} \bar{\mathbf{G}}_\mathbf{E} \mathbf{f_E} \ . \tag{11}$$

4 Integral formulations for viscoelastic materials based on the BEM

To write the BEM viscoelastic formulation based on the Kelvin-Voigt model, Eq. (4) is applied in Eq. (6), which leads to:

$$\int_\Gamma u^*_{ki} p_i d\Gamma - \int_\Omega \varepsilon^*_{kij} D_{ijlm} \varepsilon_{lm} d\Omega - \int_\Omega \varepsilon^*_{kij} \gamma D_{ijlm} \dot{\varepsilon}_{lm} d\Omega + \int_\Omega u^*_{ki} b_i d\Omega = 0 \ . \tag{12}$$

By applying the divergence theorem and replacing the stress-strain, the strain-displacement and the Cauchy formula, one can write the Eq. (13) as the BEM singular form for the viscoelastic formulation. More details of this passage can be found in Mesquita and Coda [11].

$$c_{ki}\left[u_i + \gamma \dot{u}_i\right] + \int_\Gamma p^*_{ki} u_i d\Gamma + \gamma \int_\Gamma p^*_{ki} \dot{u}_i d\Gamma = \int_\Gamma u^*_{ki} p_i d\Gamma + \int_\Omega u^*_{ki} b_i d\Omega \ . \tag{13}$$

Where $\dot{u}_i$ is the temporal derivative of displacements and the free term c_{ki} is equal to the Kronecker operator (δ_{ki}) multiplied by 0.5, for points at smooth contours, and equal to δ_{ki}, for internal points.

When introducing the numerical approximation, shape functions approximate displacement and tractions. High order polynomial functions may be adopted, by using high order boundary elements. Thus, Eq. (13) can be written for boundary nodes, in its algebraic form, as follows:

$$\mathbf{H u}(t) + \gamma \mathbf{H \dot{u}}(t) = \mathbf{G p}(t) + \bar{\mathbf{B}} \mathbf{b}(t) \ . \tag{14}$$

In which matrix $\mathbf{H}$ contains the integration kernels p^*_{ij}, matrix $\mathbf{G}$ contains the integration kernels u^*_{ij} and matrix $\bar{\mathbf{B}}$ contains the integration of u^*_{ij} over the domain Ω. Vectors $\mathbf{u}(t)$ and $\mathbf{p}(t)$ contain the displacements and tractions values, as a function of time, and the dot symbol represents its temporal derivative.

In the process of evaluating the boundary nodes, the integration kernels in the matrixes $\mathbf{H}$ and $\mathbf{G}$ of Eq. (14) become singular when the source point coincides with the field point. So, a mathematical technique must be used to evaluate this expression, as shown in Aliabadi, Hall and Phemister [21]. The singular kernels are subtracted by a Taylor expansion function and then evaluated as a Cauchy principal value.

The time-differential equation showed in Eq. (14) can be solved by the forward finite differences technique. Such technique considers a linear approximation for evaluating the first time derivative terms, as follows:

$$\dot{\mathbf{u}}(t) = \frac{\mathbf{u}^{t+1} - \mathbf{u}^{t}}{\Delta t} \quad . \tag{15}$$

Where $t+1$ represents the present time instant and Δt is the adopted time step. Thus, the analysis is divided into finite time steps and Eq. (14) turns into a time marching process:

$$\left(1 + \frac{\gamma}{\Delta t}\right)\mathbf{H}\mathbf{u}^{t+1} = \frac{\gamma}{\Delta t}\mathbf{H}\mathbf{u}^{t} + \mathbf{G}\mathbf{p}^{t+1} + \bar{\mathbf{B}}\mathbf{b}^{t+1} \quad . \tag{16}$$

In which the vectors **u** and **p** represent displacements and traction values at a given time step.

5 The coupling technique

Consider a two-dimensional domain Ω with contour Γ, represented by boundary elements of any order. The reinforcements are immersed in Ω and positioned over the line $\bar{\Gamma}$, which is also represented by boundary elements. The coupling technique is based on analyzing the structural elements disconnectedly, wherein one's effect in each other is an adherence force (contact force), as shown in Fig. 2.

One considers a perfect bounding contact between matrix (domain) and reinforcements. The adherence force is modelled as a one-dimensional distributed load along the reinforcement's line, named as load line. Then, the displacement compatibility and force equilibrium expressions are defined as follows:

$$\begin{aligned} \mathbf{u}_{\mathbf{E}} &= \mathbf{u}_{\mathbf{D}} \\ \mathbf{f}_{\mathbf{E}} &= -\mathbf{f}_{\mathbf{D}} \end{aligned} \quad . \tag{17}$$

Where $\mathbf{u}_{\mathbf{E}}$ and $\mathbf{u}_{\mathbf{D}}$ are vectors containing nodal displacements for reinforcement and matrix, respectively, $\mathbf{f}_{\mathbf{E}}$ and $\mathbf{f}_{\mathbf{D}}$ are nodal values of the distributed contact force at the reinforcement elements and at the force line in the 2D domain, respectively.

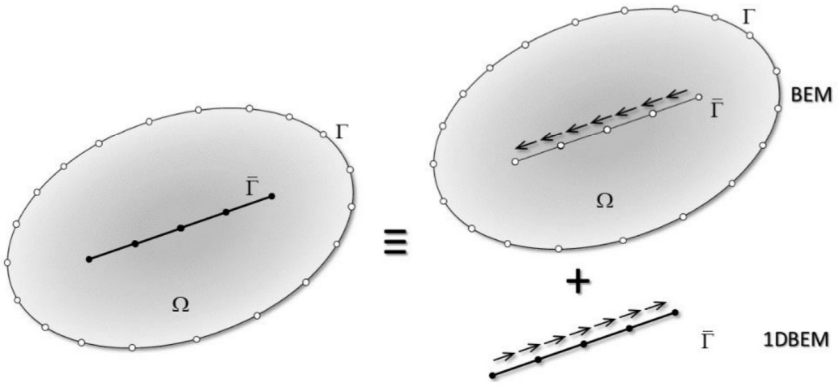

Figure 2: Matrix/reinforcement coupling technique.

The contact force at the load line in the 2D domain is considered as a body force in the BEM formulation. Thus, the domain integral term, given by the expression $\bar{\mathbf{B}}\mathbf{b}^{t+1}$ in Eq. (16), is degenerated and evaluated along a line integral. Hence, all integrals of the singular form can be evaluated as line integrals, without the need for domain mesh or cells. Equation (16) can be rewritten for the boundary

points as:

$$(1+\alpha)\mathbf{H_{CC}u_c} = \mathbf{G_{CC}p_c} + \mathbf{G_{CF}f_D} + \alpha\mathbf{H_{CC}}\bar{\mathbf{u}}_\mathbf{c} \ . \tag{18}$$

Where subscripts **C** and **F** of the matrixes **H** and **G** indicate, respectively, the integral results of the fundamental solutions over the boundary elements and over the reinforcement elements. Vectors $\mathbf{u_c}$ and $\mathbf{p_c}$ contain displacement and traction values at the boundary points; α parameter is equal to the relation $\gamma/\Delta t$ and the bar symbol above the displacement vector ($\bar{\mathbf{u}}_\mathbf{c}$) represents its value in the previous time step.

Then, the BEM singular form is evaluated for the reinforcement's nodes, as internal points into the domain. Equation (13) must be applied for internal points, making the free term $c_{ki} = \delta_{ki}$, multiplied by the displacements and its temporal derivative (u_i and $\dot{u}_i$) of the internal point. Hence, considering the load line as a body force, applying numerical approximation and replacing Eq. (15), one can rewrite Eq. (13) for internal points, in its algebraic form, as follows:

$$(1+\alpha)\mathbf{u_E} + (1+\alpha)\mathbf{H_{FC}u_c} = \mathbf{G_{FC}p_c} + \mathbf{G_{FF}f_D} + \alpha\mathbf{H_{FC}}\bar{\mathbf{u}}_\mathbf{c} + \alpha\bar{\mathbf{u}}_\mathbf{D} \ . \tag{19}$$

The reinforcements are assumed as linear elastic time independent. Thus, Eq. (11) is utilized to describe the relation between $\mathbf{u_E}$ and $\mathbf{f_E}$ through the mechanical behavior of the reinforcements. This equation can be rewritten as follows:

$$\mathbf{K_F u_E} = \mathbf{G_F f_E} \ . \tag{20}$$

Since the matrixes $\mathbf{K_F}$ and $\mathbf{G_F}$ are given by:

$$\begin{aligned} \mathbf{K_F} &= (\mathbf{G_E})^{-1}\mathbf{H_E} \\ \mathbf{G_F} &= (\mathbf{G_E})^{-1}\bar{\mathbf{G}}_\mathbf{E} \end{aligned} \ . \tag{21}$$

One can notice that Eq. (20) could also represent the one-dimensional FEM, by making $\mathbf{K_F}$ the stiffness matrix and $\mathbf{G_F}$ the lumping matrix, which transforms the distributed applied force into equivalent concentrated nodal forces. Therefore, the present formulation describes both couplings 1DBEM/BEM and FEM/BEM.

Finally, the relations from Eq. (17) are applied in Eq. (18), Eq. (19) and Eq. (20), resulting in the system of equations:

$$\begin{bmatrix} (1+\alpha)\mathbf{H_{CC}} & \mathbf{0} & -\mathbf{G_{CF}} \\ (1+\alpha)\mathbf{H_{FC}} & (1+\alpha)\mathbf{I} & -\mathbf{G_{FF}} \\ \mathbf{0} & \mathbf{K_F} & \mathbf{G_F} \end{bmatrix} \begin{Bmatrix} \mathbf{u_c} \\ \mathbf{u_D} \\ \mathbf{f_D} \end{Bmatrix} = \begin{bmatrix} \mathbf{G_{CC}} & \alpha\mathbf{H_{CC}} & \mathbf{0} \\ \mathbf{G_{FC}} & \alpha\mathbf{H_{FC}} & \alpha\mathbf{I} \\ \mathbf{0} & \mathbf{0} & \mathbf{0} \end{bmatrix} \begin{Bmatrix} \mathbf{p_c} \\ \bar{\mathbf{u}}_\mathbf{c} \\ \bar{\mathbf{u}}_\mathbf{D} \end{Bmatrix} \ . \tag{22}$$

Where **I** is the identity matrix. After enforcing the boundary conditions, this system of algebraic equations leads to the problem solution in terms of boundary and reinforcement's displacements and tractions.

6 Numerical results

The proposed formulation is applied in the mechanical analysis of the structure illustrated in Fig. 3. The two-dimensional domain is isotropic, plane stress condition is assumed and it is reinforced by one long horizontal fiber. The figure also exhibits dimensions, loads and the following physical properties: reinforcements' area (A), Young's modulus (E) and Poisson's ratio (ν) of the 2D domain. The loads illustrated in Fig. 3 are constant in time and all initial conditions are null.

The boundary element mesh is composed of 34 quadratic elements at the boundary of the 2D

domain and 50 quadratic reinforcement's elements at the long fiber's line. Therefore, the entire model consists of 346 degrees of freedom. A prior analysis has certified the mesh convergence for this model, i.e., the refinement of the contour elements mesh is adequate for this problem. The convergence of the time marching process will be exhibited in this example by using three different time steps:

- Δt_1 = 16.67 hours (approximately 0.7 days);
- Δt_2 = 66.67 hours (approximately 2.8 days);
- Δt_1 = 666.67 hours (approximately 28 days);

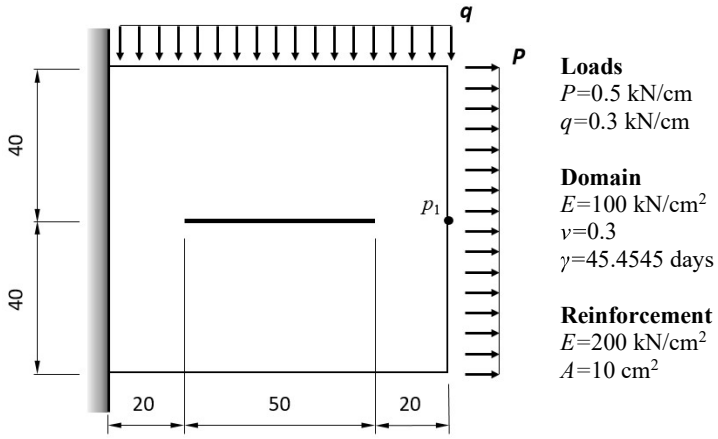

Figure 3: Geometry and physical properties (dimensions in cm).

To validate the results obtained by the proposed formulation, a model is constructed in the software ANSYS, since analytical solutions are not easily found for reinforced domains. The model is composed by 1800 solid two-dimensional elements (*PLANE*182) and 50 truss one-dimensional elements (*LINK*180). ANSYS approach is based on a pure FEM formulation, wherein the reinforcements must have coincident nodes with the domain mesh. The viscoelastic behavior of the matrix is modelled by using a transient solution, in which the 2D domain material model has a damping behavior linearly proportional to the stiffness by a coefficient γ. The mechanical behavior of this damped model over time is the same as the viscoelastic model, since the damping matrix coincides with the Kelvin-Voigt constitutive matrix. The time transient analysis was set to finish at 270 days with time steps of 0.7 days (approximately 16 hours). The FE model, of 3772 degrees of freedom, has shown convergence and it can be used for results reference.

Figure 4 illustrates the horizontal (u_x) and vertical (u_y) displacements at the point p_1 along time obtained when the different time steps Δt_1, Δt_2 and Δt_3 are considered. The graphics also compare the results with the reference values (ANSYS). The results obtained by Δt_1 and Δt_2 are equally precise, whereas Δt_3 led to worst results, taking into account the reference values. This analysis demonstrates the convergence of the time marching process, in terms of time step. In addition, one observes the asymptotic behavior of the viscoelastic analysis along time. As well as the damping response, the viscous response is maximum in the beginning of the analysis and decreases along time, leaving the elastic response to govern the mechanical behavior after a certain time, which can explain the asymptotic behavior. The figures also shows the perfect agreement between the results obtained with both time steps Δt_1 and Δt_2 and the reference's results.

Figure 5 shows the fiber's results through the time variation of the horizontal (u_x) and vertical (u_y) displacement at the right endpoint. This points is also the maximum displacement point. These graphics illustrate the reference results and the values obtained with Δt_1, Δt_2 and Δt_3. Similarly as the previous figure, one can observe the convergence regarding the time step size. Furthermore, the displacements exhibit an asymptotic behavior along time and one can observe the perfect concordance of the proposed model with the reference. Considering Fig. 5 and Fig. 6, one can verify that both time

steps Δt_1 and Δt_2 are adequate to provide correct results about this numerical example. Therefore, Δt_3 will be disregarded in the next results.

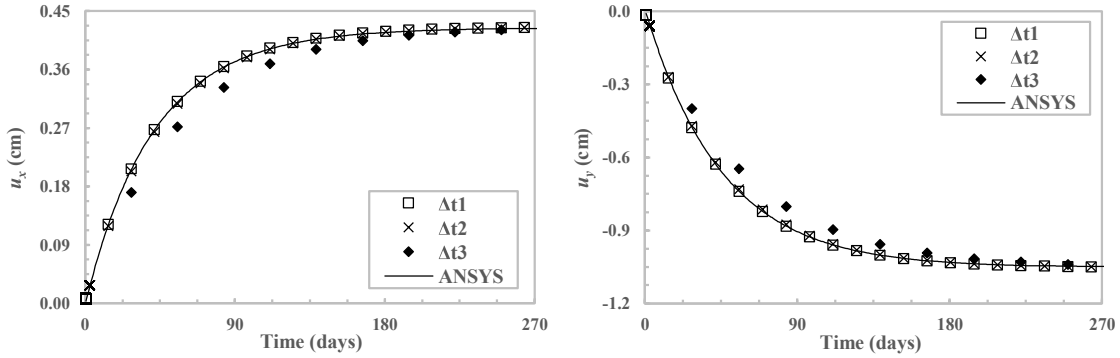

Figure 4: Horizontal (u_x) and vertical (u_y) displacements at point p_1.

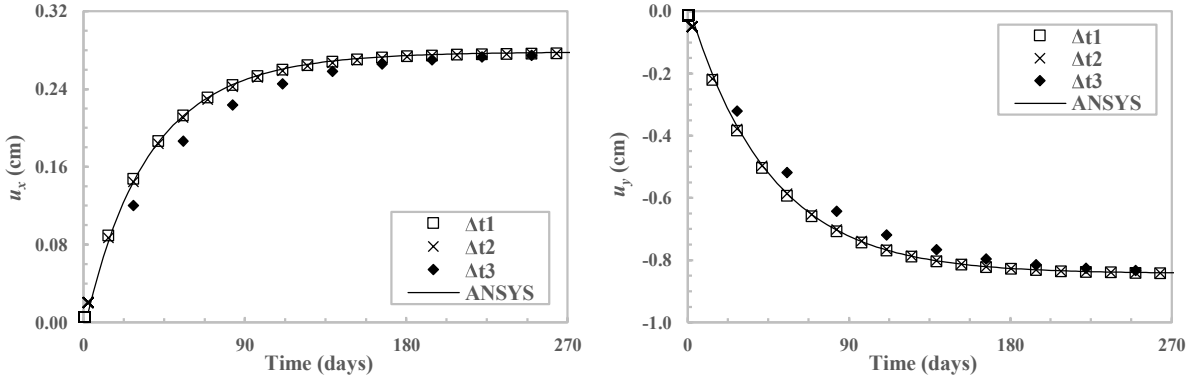

Figure 5: Horizontal (u_x) and vertical (u_y) displacements at the reinforcement right endpoint.

Figure 6 illustrates the horizontal (u_x) and vertical (u_y) displacements at the boundary obtained at the last time step of the analysis (270 days), using Δt_2. These graphics also exhibit the reference results (ANSYS). Variable S represents the geometry perimeter, which starts at the bottom left point and grows counter clockwise. This figure shows a perfect agreement in the proposed model results and the reference, for all the domain boundary points.

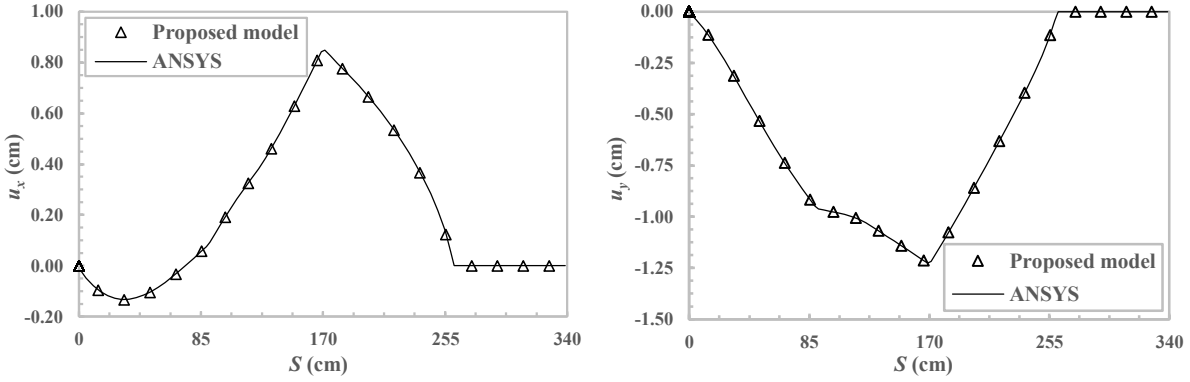

Figure 6: Horizontal (u_x) and vertical (u_y) displacements at the boundary nodes after 270 days.

Figure 7 illustrates the fiber's results for axial internal force (N), by its variation along time at the centerpoint (7-a) and its variation along the fiber's line at the last time step, 270 days (7-b). The

centerpoint is also the maximum axial force point, at all time steps of the analysis. These results were obtained considering Δt_2, since the previous analysis demonstrated the convergence of the time marching process. These graphics show a perfect agreement between the proposed model and the reference (ANSYS), as expected. By analyzing the axial force along time in Fig. 7-a, one observes that it starts in nil value and grow along time. This behavior is explained by the purely elastic response of the reinforcements, since in the beginning of the analysis the mechanical response of the structure is primarily viscous, so the reinforcement response follow the elastic response of the domain.

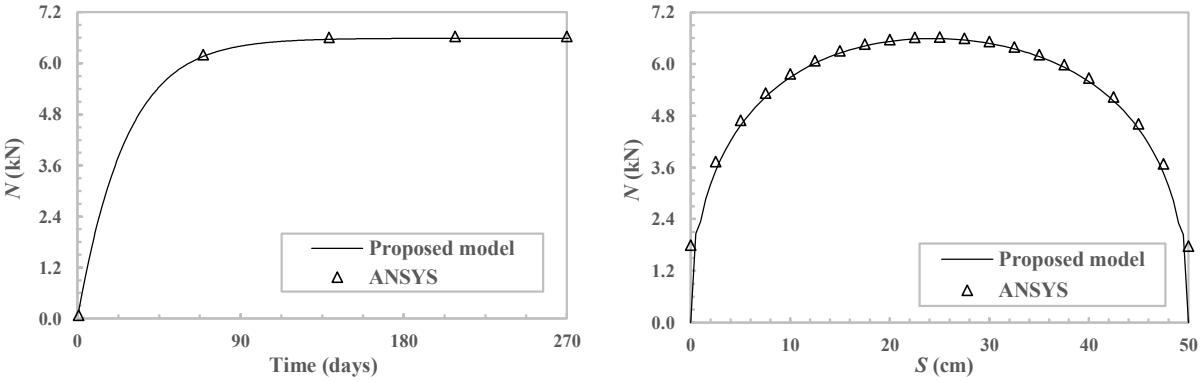

Figure 7: Axial force along time at reinforcement centerpoint (a) and axial force along the reinforcement line at the last time step (b).

In addition, Fig. 7-b also shows a smooth variation of the axial force values along the reinforcement line, with its maximum value at the centerpoint. Despite the endpoints, the axial force agrees with the reference along the reinforcement line, however, one can notice the nil value obtained by the proposed model at the reinforcement endpoints, which is not observed in the reference results. The proposed model always lead to nil axial force at reinforcements endpoints, since the domain BEM formulation does not admit concentrated forces applied into the domain, so a no null axial force at the reinforcement endpoint could not be transmitted to the matrix. On the other hand, the pure FEM formulation with coincident nodes utilized by ANSYS admits to apply concentrated forces inside the domain, which allows the force transmission from the reinforcement endpoint to the matrix. By analyzing the two-dimensional physical model, one can verify that the BEM assumption is more reliable, justifying the different results obtained at these points when comparing with the ANSYS results.

Figure 8 exhibits horizontal displacements (u_x) and internal axial force (N) over the reinforcement line (S) for different times. The graphics illustrate the results on five times (t1, t2, t3, t4 and t5), which are equally spaced in the total time analysis (1, 25, 50, 75 and 100 time steps), when Δt_2 is used. These results have already been validated by the previous graphics and analysis, therefore, Fig. 8 only exhibits the proposed model results. One observes, for all the reinforcements points, that the results start with small values and tend to converge along time, because the difference in values decreases along the specific times illustrated. This characteristic endorse the asymptotic behavior of displacements and axial force along time at all reinforcements points, as well as Fig. 4, Fig. 5 and Fig. 6 highlighted for some points. Besides, one can notice the same behavior of Fig. 7-a for all reinforcements points, due to its purely elastic response.

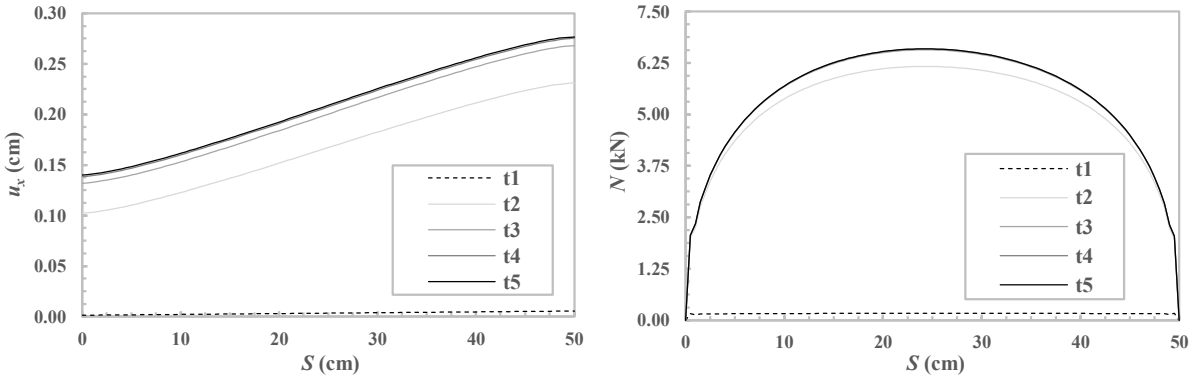

Figure 8: Horizontal displacements (u_x) and axial force (N) of reinforcement over its line for different time steps.

7 Conclusions

This study presented a coupling formulation for the mechanical analysis of reinforced viscoelastic materials. The Kelvin-Voigt model was used to represent the linear viscoelastic behavior of the matrix by the singular 2D BEM formulation. Nevertheless, complex rheological approaches, such as Maxwell and Boltzmann may be fast implemented. This approach of the BEM is efficient and accurate to represent the material time dependent behavior, without the need for cells, domain mesh or residual decaying forces based on relaxation functions, which could make the application of the boundary method more complex. To represent reinforced media, a coupling technique based on the BEM/BEM scheme was utilized, using a one-dimensional singular BEM approach not very common in literature, for which the fundamental solution for displacement and axial force was presented. The formulation of the coupling method, based on force equilibrium and displacement compatibility is simple and easy to implement. This approach allows writing the BEM model formulation considering only boundary integrals. By the results achieved in the numerical example, this approach can be considered efficient, robust and accurate. The numerical application showed excellent agreement among the responses and the reference results. The coupling formulation leads to the stable results, in which oscillating forces at the reinforcements end were not observed in any step of the viscoelastic time marching process. The results also showed no problems regarding convergence for the present formulation. Therefore, the proposed formulation has large potential for solving complex structural problems and for being used in future developments.

Acknowledgements

Sponsorship of this research project by the São Paulo State Foundation for Research (FAPESP), Project Number 2018/20253-4 is greatly appreciated.

References

[1] E. Armentani R. and Citarella, 2006, “DBEM and FEM analysis on non-linear multiple crack propagation in an aeronautic doubler-skin assembly”, International Journal of Fatigue, 28(5-6), 598-608.
[2] R. Citarella, 2009, “Non-linear MSD crack growth by DBEM for a riveted aeronautic reinforcement”, Advances in Engineering Software, 40(4), 253-259.
[3] H.L. Oliveira and E.D. Leonel, 2017, “A BEM formulation applied in the mechanical material modelling of viscoelastic cracked structures”, International Journal of Advanced Structural Engineering, 9(1), 1-12.

[4] J.T. Chern, 1993, "Finite element modeling of viscoelastic materials on the theory of fractional calculus", Ph.D. thesis, Pennsylvania State University, USA, 1993.
[5] S. Shaw, M.K. Warby J.R. and Whitman, 1997, "Error estimates with sharp constants for a fading memory Volterra problem in linear solid viscoelasticity", SIAM J. Numer. Anal. 34, 1237–1254.
[6] F.J. Rizzo and D.J. Shippy, 1971, "An application of the correspondence principle of linear viscoelasticity theory", SIAM J Appl Math 21(2):321–330.
[7] Y. Liu and H. Antes, 1997, "Application of visco-elastic boundary element method to creep problems in chemical engineering structures", Int J Pressure Vessels Piping 70:27–31.
[8] S.S. Lee and R.A. Westmann, 1995, "Application of high-order quadrature rules to time-domain boundary element analysis of viscoelasticity", Int J Numer Meth Eng 38:607–629.
[9] A.D. Mesquita and H.B. Coda, 2001, "An alternative time integration procedure for Boltzmann viscoelasticity: a BEM approach", Comput Struct 79(16):1487–1496.
[10] A.D. Mesquita and H.B. Coda, 2002, "Boundary integral equation method for general viscoelastic analysis", Int J Solids Struct 39:2643–2664.
[11] A.D. Mesquita and H.B. Coda, 2003a, "A simple Kelvin and Boltzmann viscoelastic analysis of three-dimensional solids by the boundary element method", Eng Anal Boundary Elem 27:885–895.
[12] O.C. Zienkiewicz, D.W. Kelly and Bettess, P., 1977, "The coupling of the finite element method and boundary solution procedures", International journal for numerical methods in engineering, 11(2), 355-375.
[13] S. Ganguly, J.B. Layton C. and Balakrishna, 2000, "Symmetric coupling of multi-zone curved Galerkin boundary elements with finite elements in elasticity", International Journal for Numerical Methods in Engineering, 48(5), 633-654.
[14] W.M. Elleithy, M. Tanaka A. and Guzik, 2004, "Interface relaxation FEM–BEM coupling method for elasto-plastic analysis", Engineering Analysis with Boundary Elements, 28(7), 849-857.
[15] R.A. Bia, Z. Ostrowski, A.J. Kassab, Q. Yin and E. Sciubba, 2002, "Coupling BEM, FEM and analytic solutions in steady-state potential problems", Engineering analysis with boundary elements, 26(7), 597-611.
[16] A.D. Mesquita and H.B. Coda, 2003b, "New methodology for the treatment of two dimensional viscoelastic coupling problems", Computer methods in applied mechanics and engineering, 192(16-18), 1911-1927.
[17] L.P. Buffon, 2018, "Boundary Element Method formulations for non-homogeneous reinforced plane domains mechanical analysis", 143 p., Dissertation (M. Sc. in Civil Engineering (Structures)) – Department of Structural Engineering, São Carlos School of Engineering, University of São Paulo, São Carlos, 2018.
[18] N.W. Tschoegl, 1989, "The phenomenological theory of linear viscoelastic behavior: an introduction", Springer-Verlag, Berlin.
[19] C.A. Brebbia, J.C.F. Telles and L.C. Wrobel, 2012. Boundary element techniques: theory and applications in engineering. Springer Science & Business Media.
[20] C.A. Brebbia and J. Dominguez, 1989, "Boundary Elements: An introductory Course", New York: McGraw Hill, vol. I.
[21] M.H. Aliabadi, W.S. Hall and T.G. Phemister, 1985, "Taylor expansions for singular kernels in the boundary element method", International Journal for Numerical Methods in Engineering, 21(12), 2221-2236.